Romanian Reports in Physics, Vol. 63, No. 4, P. 1061–1069, 2011

A STUDY OF DYNAMIC CHARACTERIZATIONS OF GaAs/ALGaAs SELF-ASSEMBLED QUANTUM DOT LASERS

H. ARABSHAHI

Payame Nour University of Fariman, Department of Physics, Fariman, Iran
E-mail: hadi_arabshahi@yahoo.com

Received September 28, 2010

*Abstract***.** In this research we have solved the rate equations for GaAs/AlGaAs self-assembled quantum dot laser with considering the homogeneous and inhomogeneous broadening of the optical gain using fourth order Runge-Kutta method. With increasing the full width at half maximum (FWHM) of homogeneous broadening, the threshold current, turn-on delay and steady-state photons increase because of increasing the density of states in the central group. Our calculation results show also that the simulated self-assembled dot laser reaches the steady-state faster and the lasing emission is not single mode due to the gain saturation.

*Key words***:** self-assembled quantum dot laser, Runge-Kutta method, gain saturation.

1. INTRODUCTION

Broadband light-emitting devices, such as super luminescent diodes (SLDs) and external cavity tunable lasers are ideal optical sources for applications in many areas. For example, SLDs can be used in the fields of optical coherence tomography (OCT), fiber-optic gyroscope (FOG) and wavelength-division-multiplexing (WDM) system; while external cavity tunable lasers are used in the fields of optical spectroscopy, biomedical, metrology and dense wavelength division multiplexing (DWDM). It was proposed that the characteristic of size inhomogeneity naturally occurred in self-assembled quantum dots (QDs) grown by Stranski-Krastanow (SK) mode is beneficial to broadening the material gain spectra [1]. Broadband emitting QD-SLDs and broadband tuning external cavity tunable lasers with QD gain devices have been studied [2-6]. Here, we present results in broadband emitting QD material laser. These GaAs/AlGaAs QDs exhibit a broad photoluminescence (PL) full width at half maximum (FWHM) of 158 nm, which is much wider than that grown on GaAs buffer [5-7]. The short migration length of gallium atoms on AlGaAs surface increases the size dispersion of GaAs QDs, resulting in the broadening of optical spectrum. By optimizing the GaAs

spacer thickness of multi-stacked GaAs/AlGaAs QDs, over 150-nm PL FWHM is achieved. In this paper, considering the homogeneous and inhomogeneous broadening of the optical gain we have solved the rate equations numerically using fourth order Runge-Kutta method and analyze the dynamics characteristics of GaAs/AlGaAs SAQD-LDs [8-9]. We have shown that considering the nonlinear gain result in the dynamic characteristic of photons number at the FWHM of homogeneous broadening comparable near or equal to the FWHM of inhomogeneous broadening reaches the steady-state faster. The dynamics characteristics such as maximum of the relaxation oscillation magnitude, turn-on delay, relaxation oscillation frequency and modulation bandwidth are improved as the current is increased.

2. LINEAR AND NONLINEAR OPTICAL GAIN

Based on the density-matrix theory, the linear optical gain of QD active region is given as

$$g^{(1)}(E) = \frac{2pe^2 hN_D}{cn_r e_0 m_0^2} \cdot \frac{\left|p_{cv}^s\right|(f_c - f_v)}{E_{cv}} B_{cv}(E - E_{cv}), \tag{1}$$

where n_r is the refractive index, N_D is the volume density of QDs, $\left|P_{cv}^{\sigma}\right|^2$ is the transition matrix element, f_c is the electron occupation function of the conduction-band discrete state, f_v is that of the valence-band discrete state, and E_{cv} is the interband transition energy. The linear optical gain shows the homogeneous broadening of a Lorentz shape as

$$B_{cv}(E - E_{cv}) = \frac{hG_{cv}/p}{(E - E_{cv})^2 + (hG_{cv})^2}, \tag{2}$$

where FWHM is given as $2\hbar\Gamma_{cv}$ with polarization dephasing or scattering rate Γ_{cv}. Neglecting the optical-field polarization dependence, the transition matrix element is given as

$$\left|P_{cv}^s\right|^2 = \left|I_{cv}\right|^2 M^2, \tag{3}$$

where I_{cv} represents the overlap integral between the envelope functions of an electron and a hole, and

$$M^2 = \frac{m_0^2}{12 m_e^*} \cdot \frac{E_g(E_g + D)}{E_g + 2D/3} \tag{4}$$

as derived by the first-order k.p is the interaction between the conduction band and valence band. Here, E_g is the band gap, m_e^* is the electron effective mass, E_g is the spin-orbit interaction energy of the QD material. Equation 3 holds as long as we consider QDs with a nearly symmetrical shape [10-12]. In actual SAQD-LDs, we should rewrite the linear optical gain formula of equation 1 by taking into account inhomogeneous broadening due to the QD size and composition fluctuation in terms of a convolution integral as

$$g^{(1)}(E) = \frac{2pe^2hN_D}{cn_r e_0^2} \cdot \frac{\left|p_{cv}^s\right|^2}{E_{cv}} (f_c(E) - f_v(E)), \\ B_{cv}(E - E_c)G(E_c - E_{cv})dE_c, \tag{5}$$

where E_{cv} is the center of the energy distribution function of each interband transition, $f_c(E_c)$ is the electron occupation function of the conduction-band discrete state of the QDs with the interband transition energy of E_c, and $f_v(E_v)$ is that of the valence band discrete state. The energy fluctuation of QDs are represented by $G(E_c–E_{cv})$ that takes a Gaussian distribution function as

$$G(E_c - E_{cv}) = \frac{1}{\sqrt{2p}x_0} \exp(E_c - E_{cv})^2 / 2x_0^2, \tag{6}$$

whose FWHM is given by $G_0 = 2.35x_0$. The width G_0 usually depends on the band index c and v [5].

3. RATE EQUATIONS

The most popular and useful way to deal with carrier and photon dynamics in lasers is to solve rate equations for carrier and photons [11-14]. We consider an electron and a hole as an exciton, thus, the relaxation means the process that both an electron and a hole relax into the ground state simultaneously to form an exciton. We assume that only a single discrete electron and hole ground state is formed inside the QD and the charge neutrality always holds in each QD.

In order to describe the interaction between the QDs with different resonant energies through photons, we divide the QD ensemble into j = 1, 2,... 2M+1 groups, depending on their resonant energy for the interband transition over the longitudinal cavity photon modes. $j = M$ corresponds to the group and mode at E_{cv}. We take the energy width of each group equal to the mode separation of the longitudinal cavity photon modes which equals to

$$D_E = ch / 2n_r L_{ca}, \tag{7}$$

where L_{ca} is the cavity length. The energy of the j^{th} QDs group is represented by

$$E_j = E_{cv} - (M - j)D_E, \tag{8}$$

where $j = 1, 2, ..., 2M + 1$. The QD density j^{th} QDs group is given as

$$N_D G_j = N_D G(E_j - E_{cv})D_E. \tag{9}$$

Let N_j be the carrier number in j^{th} QDs group. According to Pauli's exclusion principle, the occupation probability in the ground state of the j^{th} QDs group is defined as

$$P_j = N_j / 2N_D V_a G_j. \tag{10}$$

The rate equations are as follows [4-8]

$$\frac{\mathrm{d}N_s}{\mathrm{d}t} = \frac{I}{e} - \frac{N_s}{\tau_s} - \frac{N_s}{\tau_{sr}} + \frac{N_w}{\tau_{we}} \tag{11}$$

$$\frac{\mathrm{d}N_w}{\mathrm{d}t} = \frac{N_s}{\tau_s} + \frac{N_j}{\tau_e D_g} - \frac{N_w}{\tau_{wr}} - \frac{N_w}{\tau_{we}} - \frac{N_w}{\tau_d}$$

$$\frac{\mathrm{d}Nj}{\mathrm{d}t} = \frac{N_w G_j}{\tau_{dj}} - \frac{N_j}{\tau_r} - \frac{N_j}{\tau_e D_j} - \frac{c\Gamma}{n_r}.g^{(1)}(E)S_m$$

$$\frac{\mathrm{d}Sm}{\mathrm{d}t} = \frac{\beta N_j}{\tau_r} + \frac{c\Gamma}{n_r}.g^{(1)}(E)S_m - S_m / \tau_p$$

Where N_s, N_w, and N_j are the carrier number in separate confinement heterostructure (SCH) layer, wetting layer (WL) and j^{th} QDs group, respectively, S_m is the photon number of m^{th} mode, where m = 1,2…2M+1, I is the injected current, G_j is the fraction of the jth QDs group type within an ensemble of different dot size populations, e is the electron charge, D_g is the degeneracy of the QD ground state without spin, β is the spontaneous-emission coupling efficiency to the lasing mode. $g_{mj}^{(1)}$ is the linear optical gain which the j^{th} QDs group gives to the m^{th} mode photons where is represented by

$$g_{mj}^{(1)}(E) = \frac{2\pi e^2 h N_D}{c n_r \varepsilon_0 e_0^2} \cdot \frac{\left| p_{cv}^s \right|^2}{E_{cv}} (2p_j - 1) \\ G_j B_{cv}(E_m - E_j). \tag{12}$$

The related time constants are as τ_s, diffusion in the SCH region, τ_{sr}, carrier recombination in the SCH region, τ_{we}, carrier reexcitation from the WL to the SCH region, τ_{wr}, carrier recombination in the WL, τ_{dj}, carrier relaxation into the j^{th} QDs group, τ_r, carrier recombination in the QDs, τ_p, photon lifetime in the cavity. The average carrier relaxation lifetime, $\overline{\tau}_d$, is given as

$$\tau_d^{-1} = \tau_{dh}^{-1} . G_n = \tau_d^{-1}(1 - P_n) G_n, \tag{13}$$

where τ_o is the initial carrier relaxation lifetime. The photon lifetime in the cavity is

$$\tau_p^{-1} = c / n_r + \ln(1 / R_1 R_2) / 2L_{cav}, \tag{14}$$

where R_1 and R_2 are the cavity mirror reflectivity, and a_i is the internal loss. The laser output power of the m^{th} mode from one cavity mirror is given a

$$I_m = h w_m c S_m \ln(1 / R) / 2L_{cav} n_r, \tag{15}$$

where w_m is the emitted photon frequency, and R is R_1 or R_2. We solved the rate equations numerically using fourth order Runge-Kutta method [13-15] to obtain the carrier and photon characteristics, and modulation response by supplying the steplike current at time $t = 0$. The system reaches the steady-state after the relaxation oscillation. We assume that all the carriers are injected into the WL, *i.e.*, $\tau_{sr} = \tau_{we} = \infty$, and consider the thermal carrier escape time $\tau_e = \infty$.

4. SIMULATION RESULTS AND DISCUSSION

We have solved the rate equations 11 using numeric method of Runge-Kutta without considering the nonlinear gain and thermal carrier escape from QDs and simulated the carrier and photon characteristics. Figure 1 shows the simulation results of carrier characteristics for different injection currents I = 1.5, 2, 2.5, 5, and 10 mA at the FWHM of homogeneous broadenings for $\hbar\gamma_{cv}$ = 10 meV.

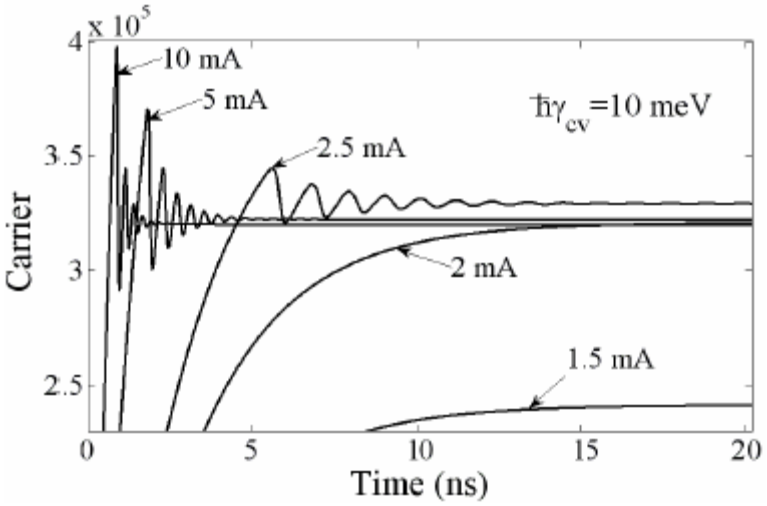

Fig. 1 – Simulation results of carrier characteristics for different injection currents of 1.5, 2, 2.5, 5, and 10 mA at the FWHM of homogeneous broadenings for 10 meV .

As shown in Fig. 1, with increasing the injection current, turn on delay decreases and maximum of the relaxation oscillation magnitude and relaxation oscillation frequency increase. Maximum of the relaxation oscillation magnitude increases and relaxation oscillation frequency decreases for the larger FWHM of homogeneous broadening.

Figure 2 shows the simulation results of photon characteristics for different injection currents $I = 2$, 2.5, 5 and 10 mA at the FWHM of homogeneous broadenings about 3, 5, 7 and 10 meV. As shown in Fig. 2, the steady-state photons are increased as the injection current is increased. This is because of increasing the injection current the carriers of QDs increase that result in increasing the cavity lasing photons, these increased photons that we call them early photons lead to increasing the stimulated emission rate as a result the QDs carriers decrease and the lasing photons increase at the new steady-state. With increasing the injection current, turn on delay decreases, this occur because the required carriers for start of the relaxation oscillation supply earlier. Relaxation oscillation frequency and maximum of the relaxation oscillation magnitude also enhance further increment of early photons lead to further increment of maximum of the relaxation oscillation magnitude. On the other side increasing the stimulated emission rate leads to the rather light amplification and decreasing the cavity photons time as a result the relaxation oscillation frequency increases and the laser reaches the steady-state earlier. As the FWHM of homogeneous broadening increases from c to f, turn on delay increases, because density of states of the central group increase as a result the required carriers for start of lasing increase and supply slower. Steady-state photons except to Fig. 3c at the current $I = 2.5$ mA increases due to increasing the QDs within the homogeneous broadening of the central mode.

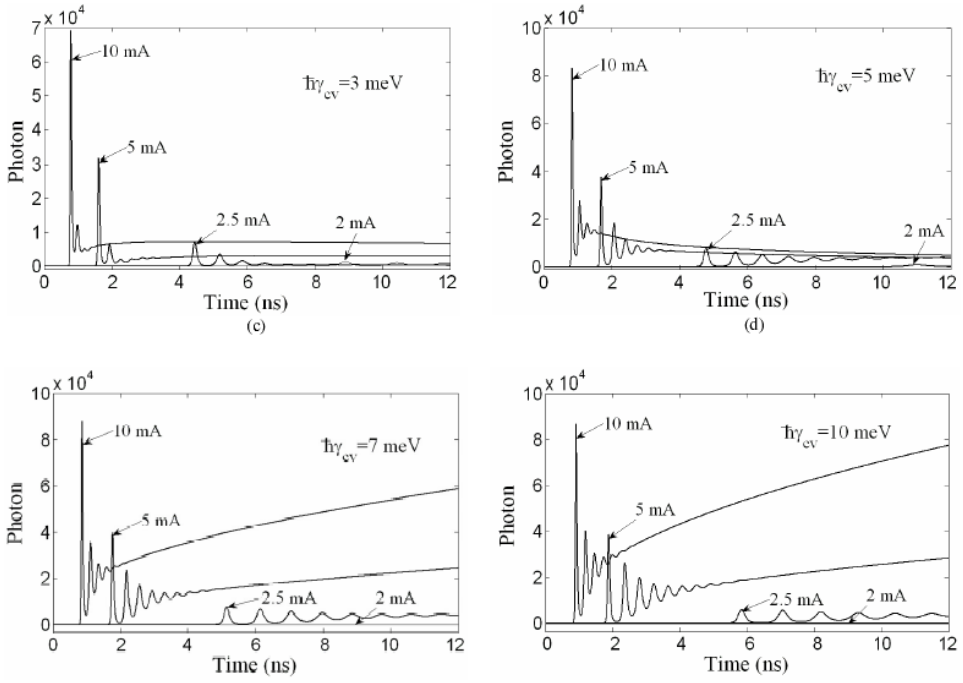

Fig. 2 – Simulation results of photon characteristics for different injection currents $I = 2$, 2.5, 5, and 10 mA when the FWHM of homogeneous broadening is 3, 5, 7 and 10 meV.

Enhancing of the homogeneous broadening until special value for the specific current (for example, in Fig. 3a, until $\hbar\gamma_{cv} = 3\,\text{meV}$ for $I = 2$ mA leads to increasing of maximum of the relaxation oscillation magnitude and the steady-state photons, because the central group DOS and thus the central group carriers enhance. Further elevating of the homogeneous broadening results in heightening of the empty DOS at the central group (decreasing of the population inversion) and slaking of maximum of the relaxation oscillation magnitude and the steady-state photons. As shown at injection current $I = 2$ mA with increasing of the FWHM of homogeneous broadening from 6 meV, the population inversion is provided at the higher current and the threshold current elevates.

Figure 4 shows other illustration from photon-characteristics for different injection currents $I = 2$, 2.5, 5, and 10 mA at (a) $\hbar\gamma_{cv} = 3\,\text{meV}$, (b) 5 meV, (c) 7 meV, and (d) 10 meV.

As shown in Fig. 4a, the steady-state photons at $I = 2.5$ mA are lesser than $I = 2$ mA. Lasing photons at $I = 5$ and 10 mA do not reach the steady state after 80 ns and 40 ns. As it is shown in Fig. 4b, the lasing photons at $I = 5$ and 10 mA decrease as the time increases and they become lesser than that of $I = 2$ mA after 45 ns, they do not reach the steady-state after 80 ns. Lasing photons at 10 mA become lesser

than that of 5 mA after 30 ns. Lasing photons at $I = 2.5$ mA increase as the time enhances, and they do not reach the steady-state after 100 ns. As it is shown in Fig. 4c, the lasing photons at $I = 2.5$ mA reach the steady-state after 80 ns, but, the lasing photons at $I = 5$ and 10 mA do not reach the steady-state and they elevate as the time increases. As it is shown in Fig. 4d, the lasing photons at $I = 5$ and 10 mA do not reach the steady-state after 300 ns. These non steady-states are due to not considering of gain saturation effect.

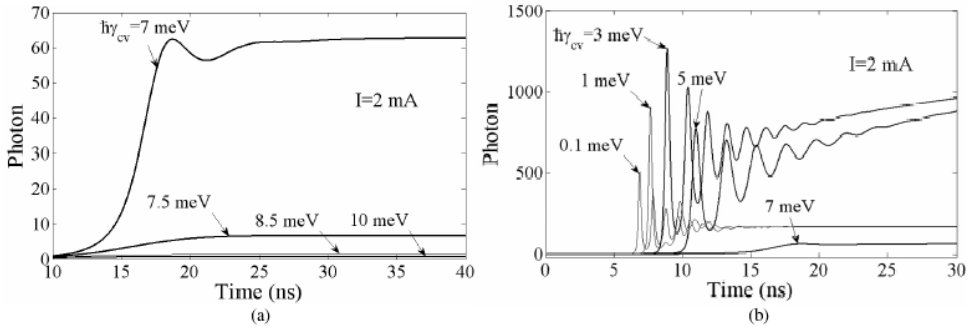

Fig. 3 – Photon-characteristics for I=2 mA at: a) $\hbar\gamma_{cv} = 7$, 7.5, 8.5, and 10 meV; b) $\hbar\gamma_{cv} = 0.1$, 1, 3, 5, and 7 meV.

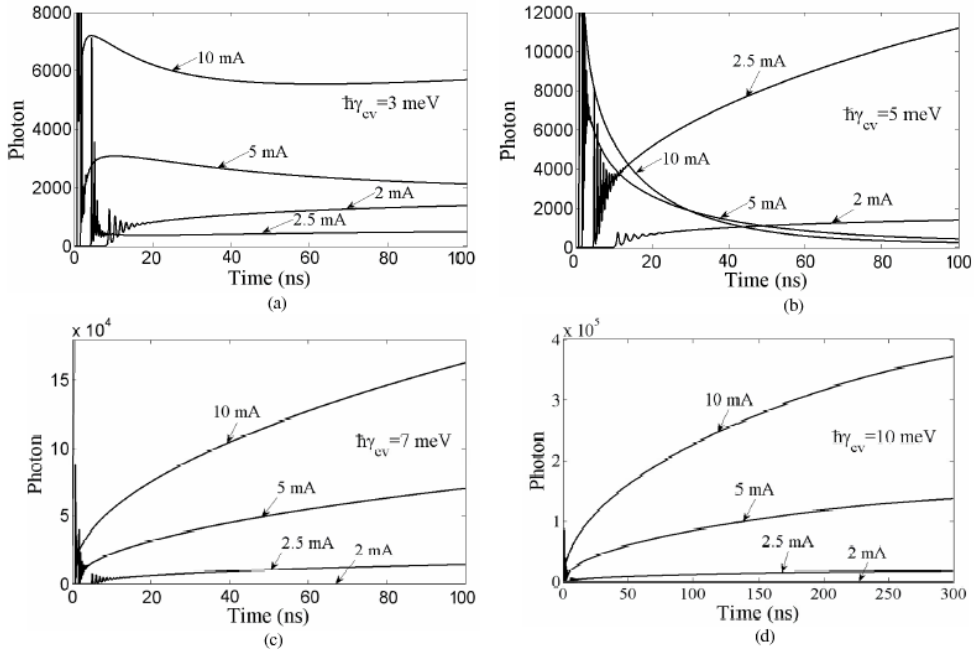

Fig. 4 – Other illustration from photon-characteristics for different injection currents $I = 2$, 2.5, 5, and 10 mA at: a) $\hbar\gamma_{cv} = 3$ meV; b) 5 meV; c) 7 meV; d) 10 meV.

5. CONCLUSION

Self-assembled quantum dots (QDs) with broadband emitting spectra, QD super luminescent diodes (SLDs) and external cavity tunable QD laser have been studied. Considering the homogeneous and inhomogeneous broadening of the optical gain without and with considering the nonlinear gain and thermal carrier escape from QDs, we have solved the rate equations numerically using fourth order Runge-Kutta method and analyzed the dynamic characteristics of GaAs/AlGaAs SAQD-LDs. Dynamic characteristics and steady-state photons improve as the current increases. Considering the nonlinear gain results in improvement of simulation results of the dynamic characteristics of GaAs/AlGaAs SAQD-LD at the FWHM of homogeneous broadening comparable near and equal to the FWHM of inhomogeneous broadening. In this case the SAQD-LD reaches the steady-state faster and the lasing emission is not single mode due to the gain saturation.

Acknowledgments. The authors would like to thank Maryam Gholvani for writing up the paper.

REFERENCES

1. Z. Z. Sun, D. Ding, Q. Gong, W. Zhou, B. Xu, and Z. G. Wang, *Quantum-dot superluminescent diode: A proposal for an ultra-wide output spectrum*, Opt. Quantum Electron., **31**, pp. 1235–1246, 1999.
2. Z. Y. Zhang, Z. G. Wang, B. Xu, P. Jin, Z. Z. Sun, and F. Q. Liu, *High performance quantum-dot superluminescent diodes*, IEEE Photon. Technol. Lett., **16**, *1*, pp. 27–29, Jan. 2004.
3. Z. Y. Zhang, R. A. Hogg, P. Jin, T. L. Choi, B. Xu, and Z. G. Wang, *High-power quantum-dot superluminescent LED with broadband drive current insensitive emission spectra using tapered active region*, IEEE Photon. Technol. Lett., **20**, *10*, pp. 782–784 2008.
4. N. Liu, P. Jin, and Z. G. Wang, *InAs/GaAs quantum-dot super luminescent diodes with 110 nm bandwidth,* Electron. Lett., **41**, *25*, pp. 1400–1402 2005.
[5. X. Q. Lv, N. Liu, P. Jin, and Z. G. Wang, *Broadband emitting super luminescent diodes with InAs quantum dots in AlGaAs matrix*, IEEE Photon. Technol. Lett., **20**, *20*, pp. 1742–1744, 2008.
6. M. Sugawara, *Self -Assembled InGaAs/GaAs Quantum Dots*, Academic Press, 60, 1999.
7. M. Sugawara, Phys. Rev. B, **61**, p. 7595, 2000.
8. A. Bilenca, IEEE J.Quantum electron, **40**, *6*, 2004.
9. C. L. Tan, Comput. Mater. Sci., 2008; doi: 10.1016/*j. commatsci.* 2008. 01.049.
10. C. L. Tan and Y. Wang, Applied Phys. Lett., **91**, p. 061117, 2007.
11. A. Markus and *et. al.*, IEEE J. Selected topics in quantum electronics, **9**, *5*, 2003.
12. M. Grundmann, *Nano Optoelectronics*, Springer, 2002.
13. M. Sugawara, Applied. Phys. Lett., **71**, p. 2791, 1997.
14. M. Sugawara, Phys. Rev. B, **51**, p. 10743, 1995.
15. L. A. coldren, *Diode Lasers and Photonic Integrated Circuits*, John Wiley & Sons Inc, 1995.
16. S. L. Chuang, *Physics of Optoelectronics Devices*, John Wiley & Sons Inc, 1995.